



Published in final edited form as:

Free Radic Res. 2015 ; 49(9): 1140–1146. doi:10.3109/10715762.2015.1050587.

***In Vivo* Targeted Molecular Magnetic Resonance Imaging of Free Radicals in Diabetic Cardiomyopathy within Mice**

Rheal A. Towner^{*,1}, Nataliya Smith¹, Debra Saunders¹, Jorge Carrizales¹, Florea Lupu², Robert Silasi-Mansat², Marilyn Ehrenshaft³, and Ronald P. Mason³

¹Advanced Magnetic Resonance Center, Oklahoma Medical Research Foundation, Oklahoma City, OK 73104 USA

²Cardiovascular Biology, Oklahoma Medical Research Foundation, Oklahoma City, OK 73104 USA

³Laboratory of Pharmacology and Chemistry, National Institute of Environmental Health Sciences, Research Triangle Park, NC 27709 USA

Abstract

Free radicals contribute to the pathogenesis of diabetic cardiomyopathy. We present a method to observe *in vivo* free radical events within murine diabetic cardiomyopathy. This study reports on *in vivo* imaging of protein/lipid radicals using molecular MRI (mMRI) and immuno-spin trapping (IST) in diabetic cardiac muscle. To detect free radicals in diabetic cardiomyopathy, streptozotocin (STZ)-exposed mice were given 5,5-dimethyl-pyrroline-*N*-oxide (DMPO) and administered an anti-DMPO probe (biotin-anti-DMPO antibody-albumin-Gd-DTPA). For controls, non-diabetic mice were given DMPO (non-disease control), and administered an anti-DMPO probe; or diabetic mice were given DMPO but administered a non-specific IgG contrast agent instead of the anti-DMPO probe. DMPO administration started at 7 weeks following STZ treatment for 5 days, and the anti-DMPO probe was administered at 8 weeks for MRI detection. MRI was used to detect a significant increase ($p < 0.001$) in MR image signal intensity (SI) from anti-DMPO nitron adducts in diabetic murine left-ventricular (LV) cardiac tissue, compared to controls. Regional increases in MR SI in the LV were found in apical and upper left areas ($p < 0.01$ for both), compared to controls. The biotin moiety of the anti-DMPO probe was targeted with fluorescently-labeled streptavidin to locate the anti-DMPO probe in excised cardiac tissues, which indicating elevated fluorescence only in cardiac muscle from mice administered the anti-DMPO probe. Oxidized lipids and proteins were also found to be significantly elevated ($p < 0.05$ for both) in diabetic cardiac muscle compared to controls. It can be concluded that diabetic mice have more heterogeneously distributed radicals in cardiac tissue than non-diabetic mice.

Keywords

Immuno-spin trapping (IST); free radical targeted imaging; *in vivo*; streptozotocin (STZ); mice

^{*}**Corresponding Author:** Rheal A. Towner, Ph.D., Director, Advanced Magnetic Resonance Center, Oklahoma Medical Research Foundation, Oklahoma City, OK USA 73104, Rheal-Towner@omrf.org, Phone: 405-271-7383.

Declaration of Interest Section

The authors declare no competing financial interests.

Introduction

Cardiovascular disease is the primary cause of morbidity and mortality among diabetics [1-3]. Diabetic cardiomyopathy is characterized by (1) early impairments in diastolic function, as measured by Doppler echocardiography; (2) development of cardiomyocyte hypertrophy; (3) myocardial fibrosis, associated with increased extracellular matrix deposition; (4) cardiomyocyte apoptosis; and (5) increased free radical generation [1,2,4]. It is thought that diabetic cardiomyopathy is initiated by alterations in energy substrates [5]. There is ample evidence from experimental studies that suggests that oxidative stress and free radicals play an important role in the pathogenesis and pathophysiology of cardiac diseases associated with diabetes [4,6-8]. The increased generation of reactive oxygen/nitrogen species (RONS) associated with diabetic cardiomyopathy is also coupled with reduced antioxidant defences and the modulation of protein signalling pathways [1]. Sources of RONS in the heart include superoxide ($O_2^{\bullet-}$) generated by NADPH oxidase (NOX) in the mitochondria, hydrogen peroxide (H_2O_2) converted to hydroxyl radicals ($\bullet OH$), and the formation of peroxynitrite ($ONOO^-$) from nitric oxide (NO) + $O_2^{\bullet-}$ [1,4]. It is also well known that hyperglycaemia [9], the fatty acid oxidation pathway, and the cytosolic storage of fatty acid and glucose/fatty acid derivatives, all promote the production of RONS [5]. Signalling cascades involved in diabetic cardiomyopathy include triggers such as hyperglycaemia, increased RAAS (rennin-angiotensin-aldosterone system) activation, altered calcium (Ca^{2+}) handling, and insulin resistance [1]. An impairment in NO signalling, associated with uncoupling of nitric oxide synthase (NOS), has also been implicated in the pathogenesis of diabetes induced myocardial damage [3,10]. There seems to be an interplay between oxidative and nitrosative/nutritive stress with cell death pathways in diabetic cardiomyopathy [11]. For example, hyperglycaemia leads to increased $O_2^{\bullet-}$, and subsequently $ONOO^-$ induces cell injury via lipid peroxidation, inactivation of enzymes and other proteins, activation of stress signalling (e.g. MMPs), triggering proapoptotic factors such as cytochrome c and caspases [11].

Traditionally, electron paramagnetic resonance (EPR) spectroscopy coupled with spin trapping (e.g. 5,5-dimethyl-1-pyrroline-*N*-oxide; DMPO) has been used in cell preparations (e.g. cells, mitochondria, endoplasmic reticulum, and peroxisomes) to detect radical adducts under physiological and pathological conditions [12,13]. From some of these studies it has been established that there are oxidatively damaged mitochondrial proteins that could play a role in oxidative stress associated with diabetes [13]. What is not well known, however, is the level of radical production and heterogeneous distribution in various organs that are affected by diabetes, including cardiac muscle.

The ability to observe oxidative stress/free radical processes *in vivo* would greatly facilitate understanding of the role of RONS in diabetic cardiomyopathy. This study reports on *in vivo* imaging of protein/lipid radicals with the use of free radical-targeted molecular MRI (mMRI) and immuno-spin trapping (IST) in cardiac muscle within diabetic mice (STZ-induced). Initially protein/lipid free radicals are trapped by DMPO (5,5-dimethyl-1-pyrroline *N*-oxide), which form DMPO-nitron radical adducts (see Fig. 1A). Once DMPO-radical adducts are formed, such as those associated with the cell plasma membranes, then the anti-

DMPO probe (biotin-anti-DMPO antibody-BSA-Gd-DTPA) which has an antibody specific for DMPO-nitron adducts (Fig. 1B) can be used to visualize *in vivo* DMPO-trapped radicals (Fig. 1C). IST was developed by Mason *et al.* as a way to bring the availability of immunological detection to the field of spin trapping [14]. Recently we used a combination of IST and molecular MRI targeting to trap and detect radicals in diabetic mouse livers, kidneys and lungs [15], septic encephalopathy [16], a mouse model for amyotrophic lateral sclerosis (ALS) [17], and in a mouse glioma model [18].

In this study we used IST combined with free radical targeted mMRI to assess diabetic cardiomyopathy in a mouse model. Verification of binding affinity of the anti-DMPO probe was obtained *in vitro* within primary cardiomyocytes that were oxidatively stressed. Fluorescence microscopy was used to verify the presence of the anti-DMPO probe in ex vivo cardiac muscle sections from diabetic mice. To support the *in vivo* findings, we also obtained ex vivo IST data verifying the presence of DMPO-nitron radical adducts, as well as identifying the presence of malondialdehyde (MDA)-adducts and 3-nitrotyrosine (3-NT), in diabetic cardiac tissue.

Methods

Synthesis of DMPO-specific MRI contrast agent

For detection of DMPO-protein/lipid radicals, a mouse monoclonal anti-DMPO antibody was used. The biotin-albumin-Gd-DTPA construct is estimated to have a MW ~80 kDa, and has an estimated 1.3 biotin and 23 Gd-DTPA groups bound to each BSA molecule [15,19,20]. A mouse mAb against DMPO-nitron adducts was conjugated via a sulfo-NHS-EDC link between the albumin and the Ab [15,19-21]. The macromolecular contrast material, biotin-BSA-Gd-DTPA, was prepared as previously described [15,19-21]. The final amount of the product, anti-DMPO-biotin-BSA-Gd-DTPA that was injected into mice was estimated to be 20 µg anti-DMPO Ab/injection, and 10 mg biotin-BSA-Gd-DTPA/injection. The estimated molecular weight of the anti-DMPO-biotin-BSA-Gd-DTPA probe (anti-DMPO probe) is estimated to be 232 kDa. As a control, normal rat-IgG (Apha Diagnostic International, San Antonio, TX, USA) conjugated to biotin-BSA-Gd-DTPA (IgG contrast agent) was synthesized by the same protocol.

STZ-induced Diabetes Model

The animal studies were conducted with approval from the Institutional Animal Care and Use Committee of the Oklahoma Medical Research Foundation. C57BL/6J mice (n=20; 6-8 weeks; Harlan Laboratories, Indianapolis, Indiana) were treated with STZ (100 mg/kg i.p./day for 2 days), and between 4-6 weeks mice were assessed for glucose levels. Severe diabetes was indicated when glucose levels were >300 mg/dl (n=10). To test for glucose, a drop of blood from the tail was put on a testing strip and read on a Bayer Ascensia Elite XL glucometer. For control groups, (1) non-diabetic mice were given DMPO (non-disease control) and administered anti-DMPO probe (n=6), (2) diabetic mice were given DMPO and administered anti-DMPO probe (n=5), or (3) diabetic mice were given DMPO but administered the non-specific IgG contrast agent (contrast agent control) instead of the anti-

DMPO probe (n=7). DMPO administration started at 7 weeks following STZ treatment. Mice were administered the anti-DMPO probe at 8 weeks following STZ treatment.

DMPO Administration

DMPO (25 μ l in 100 μ l saline) was administered i.p. 3 x daily (every 6 hours) for 5 days (i.e. 0.42 μ l DMPO/ μ l saline/day). Mice were initiated administration of DMPO 7 weeks following STZ administration, prior to injection of the anti-DMPO probe.

Treatment Groups

For control groups, (1) non-diabetic mice were given the radical trapping agent, 5,5-dimethyl-pyrroline-*N*-oxide (DMPO) (non-disease control), and administered anti-DMPO probe (n=6), (2) diabetic mice were given DMPO and administered anti-DMPO probe (n=5), or (3) diabetic mice were given DMPO but administered the non-specific IgG contrast agent (contrast agent control) instead of the anti-DMPO probe (n=7). DMPO administration started at 7 weeks following STZ treatment for 5 days, and then anti-DMPO probe was administered one week later. The contrast agent, biotin-anti-DMPO-BSA (bovine serum albumin)-Gd-DTPA, was used (200 μ g anti-DMPO and 100 μ g biotin-BSA-Gd-DTPA). Non-specific mouse-IgG conjugated to biotin-BSA-Gd-DTPA was used as a control contrast agent.

Molecular MRI

In vitro studies—Vials were prepared containing either (1) primary mouse cardiomyocytes (cells) (10^6) alone, (2) cells with DMPO + anti-DMPO probe (C + D + P), (3) cells with DMPO and hydrogen peroxide (H_2O_2) (C + D + H), (4) cells with DMPO + H_2O_2 + anti-DMPO probe (C + D + H + P), (5) cells with DMPO + H_2O_2 + IgG contrast agent (C + D + H + G), or (6) water (no cells). Isolated cardiomyocytes were used just after isolation from C57BL/6J mice (n=2). Three (3×10^6) cells were placed in 15-ml centrifuge tube with serum-free medium. DMPO (40mM) was then added. After 15 min of equilibration, H_2O_2 (50 μ M) was added. In the samples that contained all components, the anti-DMPO probe or the IgG isotype contrast agent was added (2 μ g, based on antibody calculation) 30 min later, and cells were incubated with the probe for 45 min. Following incubation, cells were collected, washed with PBS, centrifuged (500 rpm), and the pellet was resuspended in PBS for MR imaging. Each measurement was repeated 4 times per treatment group. MR images were taken using a RAREVTR (Rapid-Acquisition Relaxation Enhanced Variable Time Repetition) sequence with the following parameters: an echo time (TE) of 15 ms; repetition times (TR) of 200, 400, 800, 1200 and 1600 ms; 256 \times 256 matrix, 2 steps per acquisition, and a 1 mm slice thickness.

In vivo studies—MR experiments were carried out under general anaesthesia (1-2% Isoflurane, 0.8-1.0 L/min O_2) on a Bruker Biospec 7T/30 cm horizontal imaging spectrometer. Mice were imaged at 8 weeks following STZ administration. Anaesthetised (2% Isoflurane) restrained mice were placed in an MR probe, and their cardiac tissue (heart) was localised by MRI. Images were obtained using a Bruker S116 gradient coil (2.0 mT/m/A) and a 72 mm quadrature multi-rung RF coil. Multiple 1H -MR image slices were taken in the coronal (horizontal) plane using a gradient echo multislice (FLASH (Fast Low

Angle SHot); repetition time (TR) 250 ms, echo time (TE) 6 ms, 256×256 matrix, 2 steps per acquisition, 3×3 cm² field of view (FOV), 1 mm slice thickness) with motion suppression turned on. Mouse hearts were imaged at 0 (pre-contrast) and at 90-100 min post-contrast agent injection. Mice were injected i.v. with anti-DMPO or normal mouse IgG antibodies tagged with a biotin-Gd-DTPA-albumin-based contrast agent (200 µl/kg; 1 mg antibody/kg; 0.4 mmol Gd+3/kg) [15,19-21]. Relative MR signal intensities were calculated for selected regions-of-interest (ROIs) in the total left-ventricular region, as well as upper right, upper left, lower right, lower left and apical regions of the left ventricle (LV). Difference images were obtained by subtracting the post-contrast images (90 min after injection of the anti-DMPO probe or IgG contrast agent) from pre-contrast images.

Statistical analyses

Statistical differences between the probe-administered and control groups were analyzed with an unpaired, two-tailed Student *t* test using commercially available software (InStat; GraphPad Software, San Diego, CA, USA). A *p* value of less than 0.05 was considered to indicate a statistically significant difference.

Results

Initial *in vitro* experiments in mouse primary cardiomyocytes were conducted to establish the binding affinity of the anti-DMPO probe to oxidatively stressed cells. Figure 2 depicts both increased MRI signal intensities (SI) (Fig. 2A) and decreased T₁ relaxation times (Fig. 2B,C) in cells within vials that were exposed to H₂O₂, DMPO and the anti-DMPO probe, compared to controls. Quantitative data in Fig. 2C clearly demonstrates a significant decrease in T₁ values (sample 4; *p*<0.001) in the cells exposed to H₂O₂, DMPO and the anti-DMPO probe, compared to all other treatments (cells alone; cells exposed to H₂O₂ and DMPO; cells exposed to H₂O₂, DMPO and the IgG isotype contrast agent; or water).

For *in vivo* experiments, Figure 3A,B illustrates the sustained *in vivo* accumulation of the anti-DMPO probe in cardiac muscle (left ventricle (LV)) of diabetic mice 2 hours post-administration of the probe. There was >2-fold increase in the percent change in MRI SI in diabetic mice given DMPO and the anti-DMPO probe, compared to diabetic mice given DMPO and the IgG contrast agent (*p*<0.01) or non-diabetic mice given DMPO and the anti-DMPO probe (*p*<0.001) (Fig. 3B). Measured increases in blood glucose levels in diabetic mice are shown in Fig. 3C. For regional assessments, Figure 4 shows a significant increase in the levels of the anti-DMPO probe within the upper right and apical regions of the LV within diabetic mice given DMPO and the anti-DMPO probe (*p*<0.01 for all comparisons), compared to the controls (diabetic mice given DMPO and the IgG contrast agent, or non-diabetic mice given DMPO and the anti-DMPO probe) (Fig. 4B).

Ex vivo detection of the anti-DMPO probe in diabetic mouse hearts performed with the use of streptavidin-Cy3 which targets the biotin moiety of the anti-DMPO probe, indicated increased fluorescence compared to non-diabetic controls (Fig. 5). *Ex vivo* detection of DMPO-trapped radical adducts using IST, where diabetic and non-diabetic mouse hearts were exposed to a fluorescent-labelled anti-DMPO antibody is shown in Fig. 6, where there was increased fluorescence in the diabetic mice compared to controls.

Additional evidence of increased oxidative stress in diabetic mouse hearts is depicted in Fig. 7, where diabetic mice had increased levels of malondialdehyde (MDA) adducts (Fig. 7A) and 3-nitrotyrosine (3-NT) (Fig. 7B), compared to non-diabetic controls (both $p < 0.05$).

Discussion

Combining mMRI and with an anti-DMPO probe specific for DMPO-radical adducts and a gadolinium (Gd)-DTPA-albumin-based contrast agent for signal detection, has allowed the *in vivo* detection of signals associated with radicals in the cardiac tissue of diabetic (STZ induced) mice (Fig. 3). This study supports evidence (Fig. 3) that diabetic /cardiac tissue has more radical accumulation compared to non-diabetic cardiac tissue, detected in this study by mMRI and immuno-spin-trapping.

Molecular MRI (mMRI) relies on the specific labelling of extracellular cell surface receptors or antigens with a targeted contrast agent. The MRI contrast agent probe is targeted to a specific receptor or antigen using an antibody (Ab) which binds with high affinity to the receptor or antigen. These paramagnetic compounds alter proton magnetization relaxation times at their sites of accumulation, making them ideal for diagnostic purposes. MR contrast agents (CAs), such as paramagnetic, gadolinium (Gd)-based CAs generate a positive signal contrast (T_1 contrast), which enhances MR signal intensities of water molecules that surround the Gd-based CAs in T_1 -weighted MR images. Molecular probes, such as gadolinium (Gd)-based compounds, bound to affinity molecules, have become increasingly valuable as molecular reporting probes with the use of mMRI.

We have previously shown that free radical-targeted mMRI combined with IST could be used to detect free radical levels in the livers, lungs and kidneys of STZ-induced diabetic mice [15]. Quantitative data indicated >20-fold increase in percent change in MRI signal intensity (SI) in the livers, kidneys and lungs of diabetic mice compared to non-diabetic mice or diabetic mice given an IgG non-specific isotype contrast agent instead of the anti-DMPO probe [15]. Fluorescence imaging with streptavidin-Cy3, targeting the biotin moiety of the anti-DMPO probe in excised tissues (liver, lung and kidney), showed increased fluorescence levels for diabetic mice administered the anti-DMPO probe, compared to diabetic mice given the non-specific IgG contrast agent isotype [15]. It was also established with a fluorescent-labeled anti-DMPO antibody that diabetic mouse livers had increased levels of DMPO-trapped free radicals, compared to non-diabetic mice [15]. We had not, however, investigated the levels of *in vivo* DMPO-nitron radical adducts in cardiac muscle, which we pursued in this study. Associated with diabetic cardiomyopathy, we had shown previously that diabetic mice had significantly decreased stroke volumes, ejection fractions, fractional shortening and cardiac output, compared to non-diabetic controls, with the use of cardiac MRI [22].

As noted previously, it is well known that free radicals are involved in the pathogenesis and pathophysiology associated with diabetic cardiomyopathy [4,6-8]. Previous studies, however, have not clearly reported the level of radical production and the heterogeneous distribution of macromolecular radicals in cardiac muscle affected by diabetes. We specifically established that the left ventricular upper left and apical regions of the diabetic

cardiac muscle were found to have higher levels of DMPO-trapped free radicals (Fig. 4), compared to the same regions in appropriate controls. A recent study used clinical cardiac magnetic resonance imaging (CMR) to assess regional morphological changes associated with myocardial infarction (MI), and they indicated that there was apical ventricular rupture and an apical thrombus in the LV in a patient with MI [23]. This may suggest that there are more vulnerable regions of the LV in MI, and that possibly in diabetic cardiomyopathy that specific regions of the LV may be more prone to free radical formation. *In vivo* assessment of the radicals associated with diabetic cardiomyopathy with a targeted DMPO-nitron radical adduct molecular MRI probe allows investigators to obtain information on the heterogeneous distribution of macromolecular radicals that are formed as a result of the disease process. Although we investigated in this study the detection of radicals associated with cardiomyopathy 8 weeks following STZ induction of diabetes, the method could also be used to assess longitudinal generation of macromolecular radicals during various stages of pathogenesis. Future studies will involve *ex vivo* mass spectrometry identification of the excised diabetic cardiac muscle with high levels of macromolecular radicals (detected with the IST-mMRI method) to establish whether the radicals are of protein or lipid origin. In this study we found evidence that amounts of both oxidized proteins (e.g. 3-NT) and lipids (e.g. MDA) are elevated in diabetic cardiac muscle (Fig. 7), which may indicate that we are detecting both protein- and lipid-derived free radicals.

Conclusions

We demonstrated that diabetic (STZ induced model) mice have more radical accumulation in cardiac tissue, as measured by the presence of the anti-DMPO probe detected by molecular MRI, than non-diabetic mice, and that the level of these radicals is heterogeneously distributed. In summary, this *in vivo* imaging technique can be used to pinpoint where to further investigate the type and source of free radicals generated in oxidative stress-related diseases, such as diabetic cardiomyopathy.

Acknowledgements

This project was funded by the Oklahoma Medical Research Foundation (OMRF) (RAT), the National Institute of Environmental Health Sciences (NIEHS) (RPM), and supported by NIH grant number 5R25GM054938-10 (RAT).

References

1. Huynh K, Bernado BC, McMullen JR, Ritchie RH. Diabetic cardiomyopathy: mechanisms and new treatment strategies targeting antioxidant signaling pathways. *Pharmacology & Therapeutics*. 2014; 142:375–415. [PubMed: 24462787]
2. Bugger H, Abel ED. Molecular mechanisms of diabetic cardiomyopathy. *Diabetologia*. 2014; 57:660–671. [PubMed: 24477973]
3. Khanna S, Singh GB, Khullar M. Nitric oxide synthases and diabetic cardiomyopathy. *Nitric Oxide*. 2014; 43C:29–34. [PubMed: 25153033]
4. Liu Q, Wang S, Cai L. Diabetic cardiomyopathy and its mechanisms: role of oxidative stress and damage. *J Diabetes Investigations*. 2014; 5:623–34.
5. Lorenzo O, Ramírez E, Picatoste B, Egido J, Tuñón J. Alteration of energy substrates and ROS production in diabetic cardiomyopathy. *Mediators Inflamm*. 2013; 2013:461967. [PubMed: 24288443]

6. West IC. Radicals and oxidative stress in diabetes. *Diabetic Med.* 2000; 17:171–80. [PubMed: 10784220]
7. Lenzen S. Oxidative stress: the vulnerable beta-cell. *Biochem Soc Trans.* 2008; 36:343–7. [PubMed: 18481954]
8. Shen GX. Oxidative stress and diabetic cardiovascular disorder: roles of mitochondria and NADPH oxidase. *Can J Physiol Pharmacol.* 2010; 88:241–8. [PubMed: 20393589]
9. Adeghate E. Molecular and cellular basis of the aetiology and management of diabetic cardiomyopathy: a short review. *Mol Cell Biochem.* 2004; 261:187–91. [PubMed: 15362503]
10. Jo H, Otani H, Jo F, Shimazu T, Okazaki T, Yoshioka K, Fujita M, Kosaki A, Iwasaki T. Inhibition of nitric oxide synthase uncoupling by sepiapterin improves left ventricular function in streptozotocin-induced diabetic mice. *Clin Exp Pharmacol Physiol.* 2011; 38:485–93. [PubMed: 21554376]
11. Varga ZV, Giricz Z, Liaudet L, Hasko G, Ferdinandy P, Pacher P. Interplay of oxidative, nitrosative/nitrative stress, inflammation, cell death and autophagy in diabetic cardiomyopathy. *Biochim Biophys Acta.* 2015; 1852:232–42. [PubMed: 24997452]
12. Hawkins CL, Davies MJ. Detection and characterization of radicals in biological materials using EPR methodology. *Biochim Biophys Acta.* 2014; 1840:708–721. [PubMed: 23567797]
13. Velayutham M, Hemann C, Zweier JL. Removal of H₂O₂ and generation of superoxide radical: role of cytochrome c and NADH. *Free Radic Biol Med.* 2011; 51:160–70. [PubMed: 21545835]
14. Mason RP. Using anti-5,5-dimethyl-1-pyrroline N-oxide (anti-DMPO) to detect protein radicals in time and space with immune-spin trapping. *Free Radic Biol Med.* 2004; 36:1214–23. [PubMed: 15110386]
15. Towner RA, Smith N, Saunders D, Henderson M, Downum K, Lupu F, Silasi-Mansat R, Ramirez DC, Gomez-Mejiba SE, Bonini MG, Ehrenshaft M, Mason RP. *In vivo* imaging of immune-spin trapped radicals with molecular MRI in a mouse diabetes model. *Diabetes.* 2012; 61:2401–13.
16. Towner RA, Garteiser P, Bozza F, Smith N, Saunders D, d'Avila JCP, Magno F, Oliveira MF, Ehrenshaft M, Lupu F, Silasi-Mansat R, Ramirez DC, Gomez-Mejiba SE, Mason RP, Faria-Neto HCC. *In vivo* detection of free radicals in mouse septic encephalopathy using molecular MRI and immuno-spin-trapping. *Free Radic Biol Med.* 2013; 65:828–837.
17. Towner RA, Smith N, Saunders D, Lupu F, Silasi-Mansat R, West M, Ramirez DC, Gomez-Mejiba SE, Bonini MG, Mason RP, Ehrenshaft M, Hensley K. *In vivo* detection of free radicals using molecular MRI and immuno-spin-trapping in a mouse model for amyotrophic lateral sclerosis (ALS). *Free Radic Biol Med.* 2013; 63:351–360. [PubMed: 23722162]
18. Towner RA, Smith N, Saunders D, De Souza PC, Henry L, Lupu F, Silasi-Mansat R, Ehrenshaft M, Mason RP, Gomez-Mejiba SE, Ramirez DC. Combined molecular MRI and immuno-spin-trapping for *in vivo* detection of free radicals in orthotopic mouse GL261 gliomas. *Biochim Biophys Acta.* 2013; 1832:2153–2161. [PubMed: 23959048]
19. Towner RA, Smith N, Doblaz S, Garteiser P, Watanabe Y, He T, Saunders S, Herlea O, Silasi-Mansat R, Lupu F. *In vivo* detection of inducible nitric oxide synthase (iNOS) in rodent gliomas. *Free Radic Biol Med.* 2010; 48:691–703. [PubMed: 20034558]
20. Towner RA, Smith N, Tesiram Y, Garteiser P, Saunders D, Cranford R, Silasi-Mansat R, Herlea O, Ivanciu L, Wu D, Lupu F. *In vivo* detection of c-Met expression in a rat C6 glioma model. *J Cellular Molecular Med.* 2008; 12(1):174–186.
21. He T, Smith N, Saunders D, Doblaz S, Hoyle J, Silasi-Mansat R, Lupu F, Lerner M, Brackett DJ, Towner RA. Molecular MRI assessment of vascular endothelial growth factor receptor-2 in a rat C6 glioma model. *J Cell Molec Med.* 2011; 15:837–849. [PubMed: 20497492]
22. Yu X, Tesiram YA, Towner RA, Abbott A, Patterson E, Huang S, Garrett MW, Chandrasekaran S, Matsuzaki S, Szweda LI, Gordon BE, Kem DC. Early myocardial dysfunction in streptozotocin-induced diabetic mice. *Cardiovascular Diabetology.* 2007; 6:6. [PubMed: 17309798]
23. Waterhouse DF, Murphy T, McCarthy J, O'Neill J, O'Hanlon R. LV apical rupture complicating acute myocardial infarction: the role of CMR. *Heart Lung Circulation.* 2015 in press.

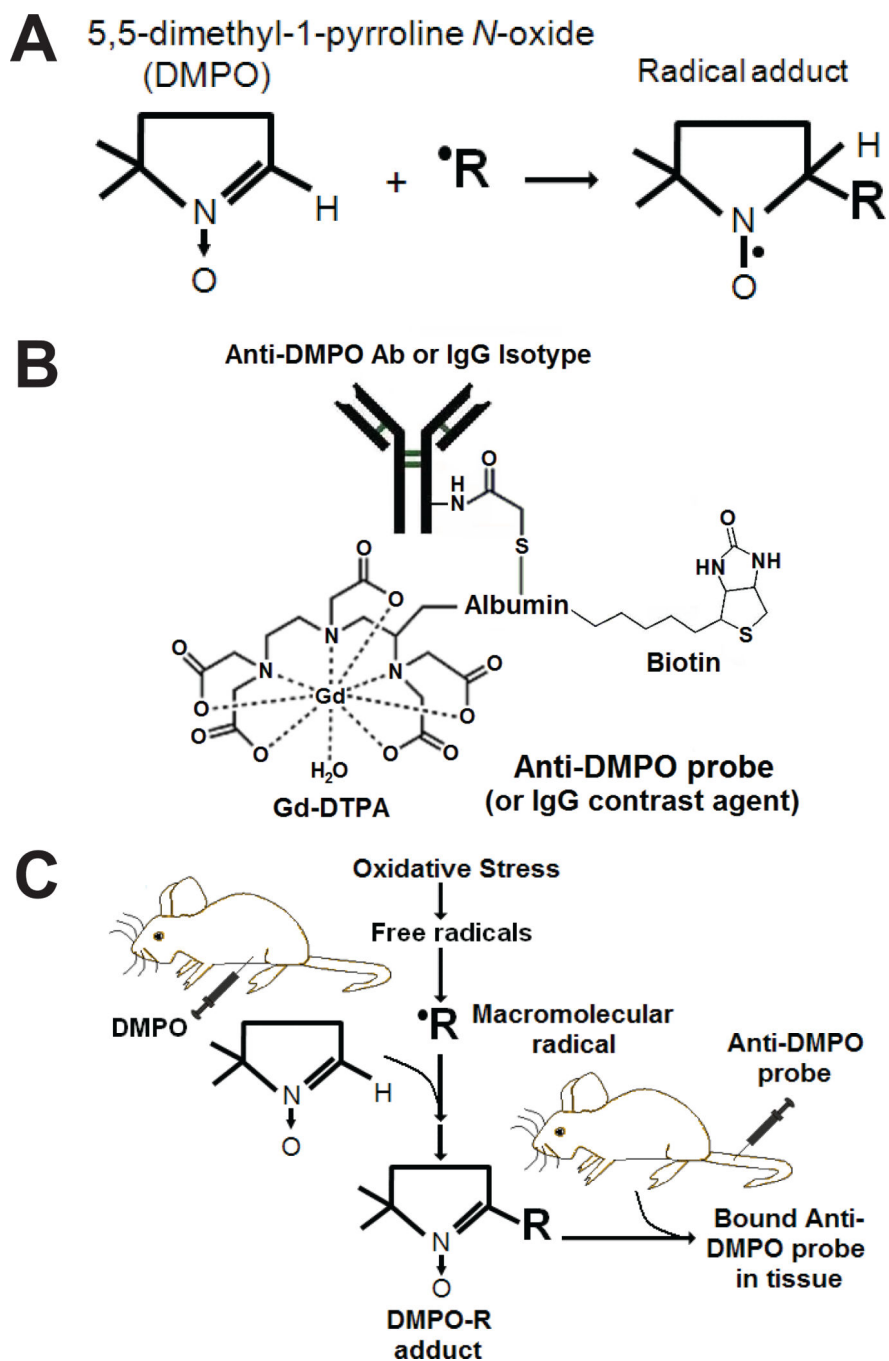


Figure 1. *In vivo* mMRI and immuno-spin-trapping (IST). (A) DMPO traps free radicals to form a stable DMPO-radical adduct complex. (B) Anti-DMPO probe (anti-DMPO antibody-albumin-Gd-DTPA-biotin) mMRI. (C) Immuno-spin trapping of free radicals ($\cdot R$) with anti-DMPO mMRI probe. DMPO is injected i.p. to trap free radicals and generate DMPO-R adducts. Anti-DMPO is injected i.v. to target DMPO-R adducts, which can be visualized by mMRI.

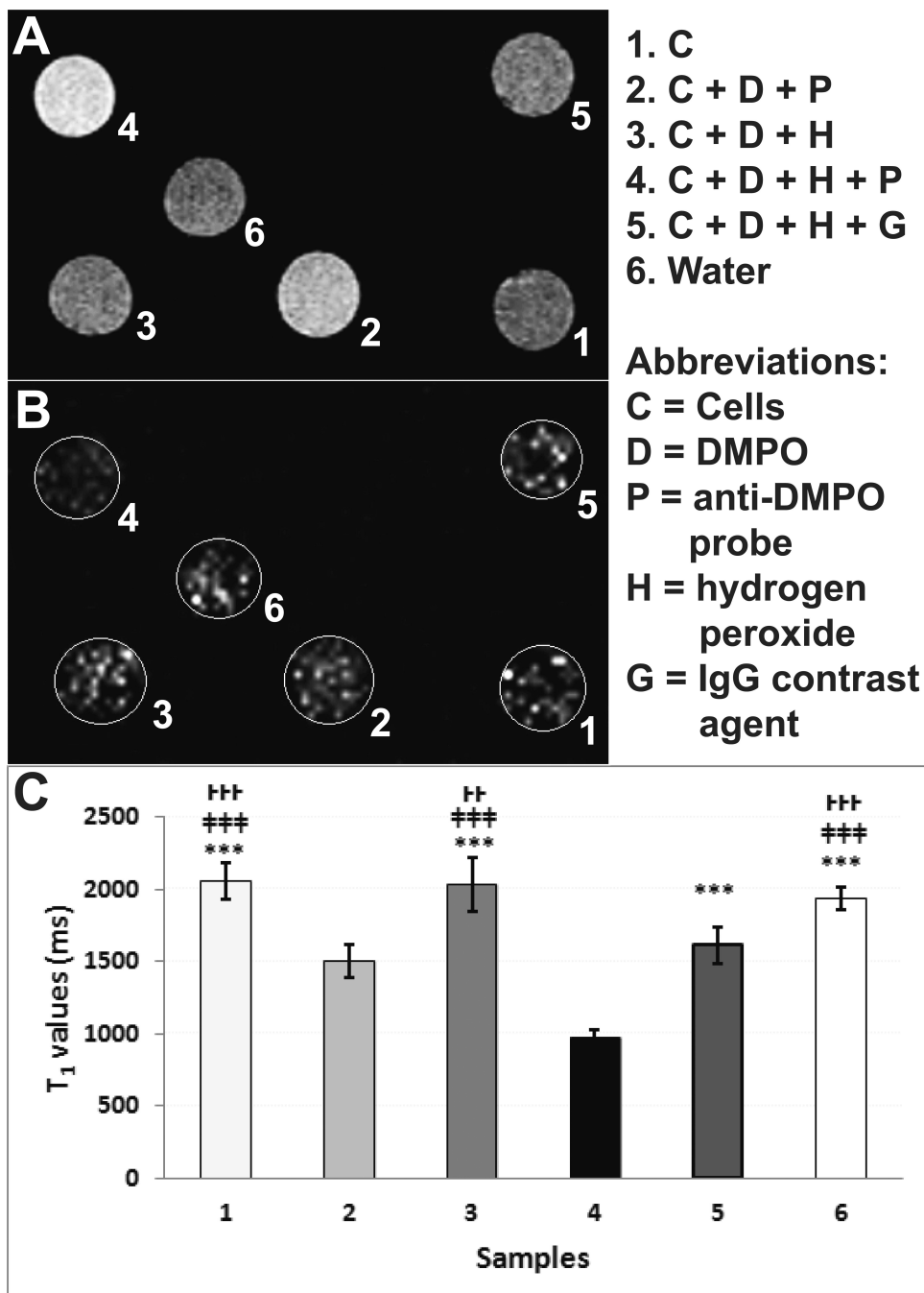


Figure 2.

In vitro assessment of the anti-DMPO probe in mouse cardiomyocytes. (A) MRI signal intensities (SI) (T_1 -w) and (B) T_1 maps of vials containing: (1) mouse cardiomyocytes, (2) cells (C) + DMPO (D) + anti-DMPO probe (P), (3) C + D + H_2O_2 (H) (C+D+H), (4) C + D + H + P, (5) C + D + H + IgG contrast agent (G), or (6) water. $n=5$ for each group. (C) T_1 relaxation values (ms) of vials containing samples 1-6. Values represented as mean \pm S.D. T_1 -w images obtained using variable TR (repetition time) spin-echo sequence. T_1 value of pixels in ROIs were calculated with the following equation: $S(TR) = S_0(1 - e^{-TR/T_1})$.

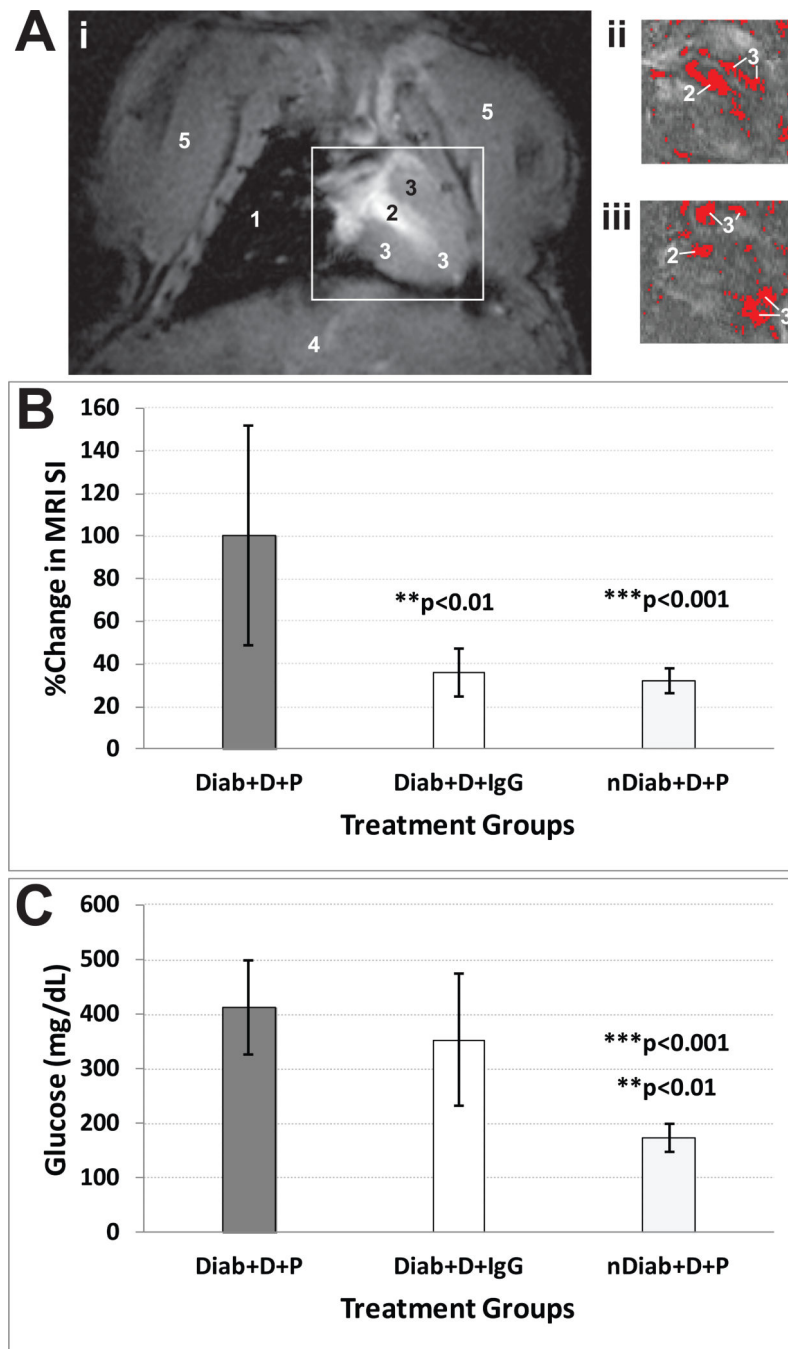


Figure 3. Molecular MRI detection of DMPO-trapped radical adducts in the left-ventricles (LV) of diabetic mice. (A) T₁-w images of STZ mouse hearts with difference images (ii and iii) obtained 90 min post-administration of anti-DMPO probe minus pre-administration image [raw MR image (i), and thresholded images (ii) and (iii)]. (B) Percent (%) change in MRI signal intensities (SI) in the left ventricle cardiac muscle of mice that were either diabetic (Diab) or non-diabetic (nDiab) and treated with DMPO (D) and either the anti-DMPO probe (P) or an IgG isotype contrast agent (IgG). There was a significant increase in MRI SI for

the diabetic mice given DMPO and the anti-DMPO probe, compared to the probe control (IgG) ($p < 0.01$) or the non-diabetic control ($p < 0.001$). (C) Blood glucose levels (mg/dL) in diabetic and non-diabetic mice. There was a significant increase in blood glucose in diabetic mice either given DMPO and the anti-DMPO probe ($p < 0.001$) or given DMPO and the IgG contrast agent ($p < 0.01$), compared to non-diabetic mice given DMPO and the anti-DMPO probe. Glucose (mg/dL) from STZ-induced diabetic mice ($n = 13$) and non-diabetic (normal). Significant differences (** $p > 0.001$ for IgG control; *** $p > 0.001$ for anti-DMPO probe) were found between IgG controls and non-diabetic anti-DMPO administered mice.

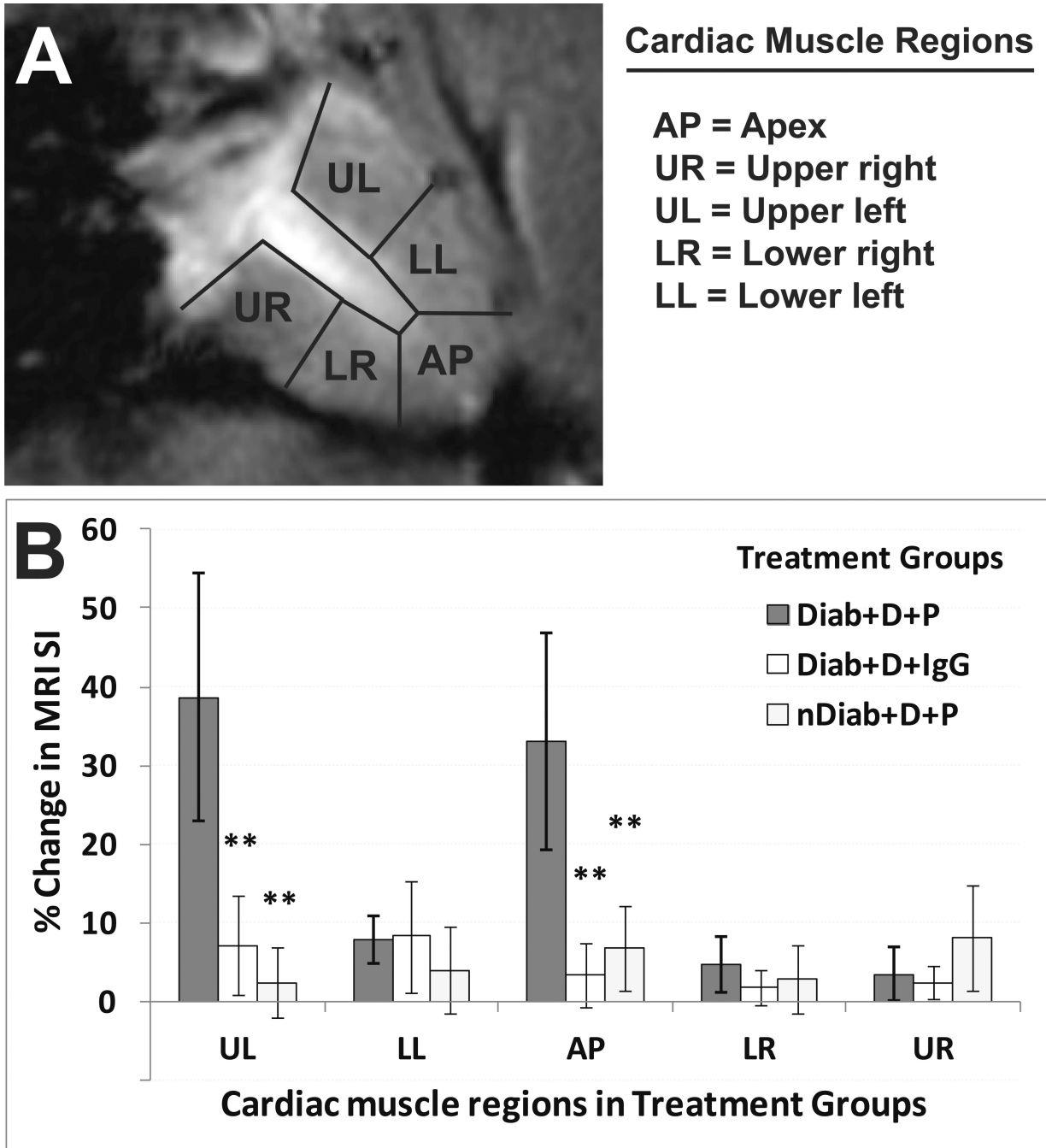


Figure 4. Regional left-ventricular (LV) molecular MRI detection of DMPO-trapped radical adducts in diabetic murine cardiac muscle. (A) T1-w image of a mouse heart with outlined segmented regions, including the apex (AP), upper right (UR), upper left (UL), lower right (LR) and lower left (LL) regions. (B) Percent (%) change in MRI signal intensities (SI) in the left ventricle cardiac muscle regions (as shown in panel A) of mice that were either diabetic (Diab) or non-diabetic (nDiab) and treated with DMPO (D) and either the anti-DMPO probe (P) or an IgG isotype contrast agent (IgG). There were significant increases in MRI SI for

the upper left and apical regions within the LV of diabetic mice given DMPO and the anti-DMPO probe (** $p < 0.01$ for all comparisons), compared to either the probe control (IgG) or the non-diabetic control.

Author Manuscript

Author Manuscript

Author Manuscript

Author Manuscript

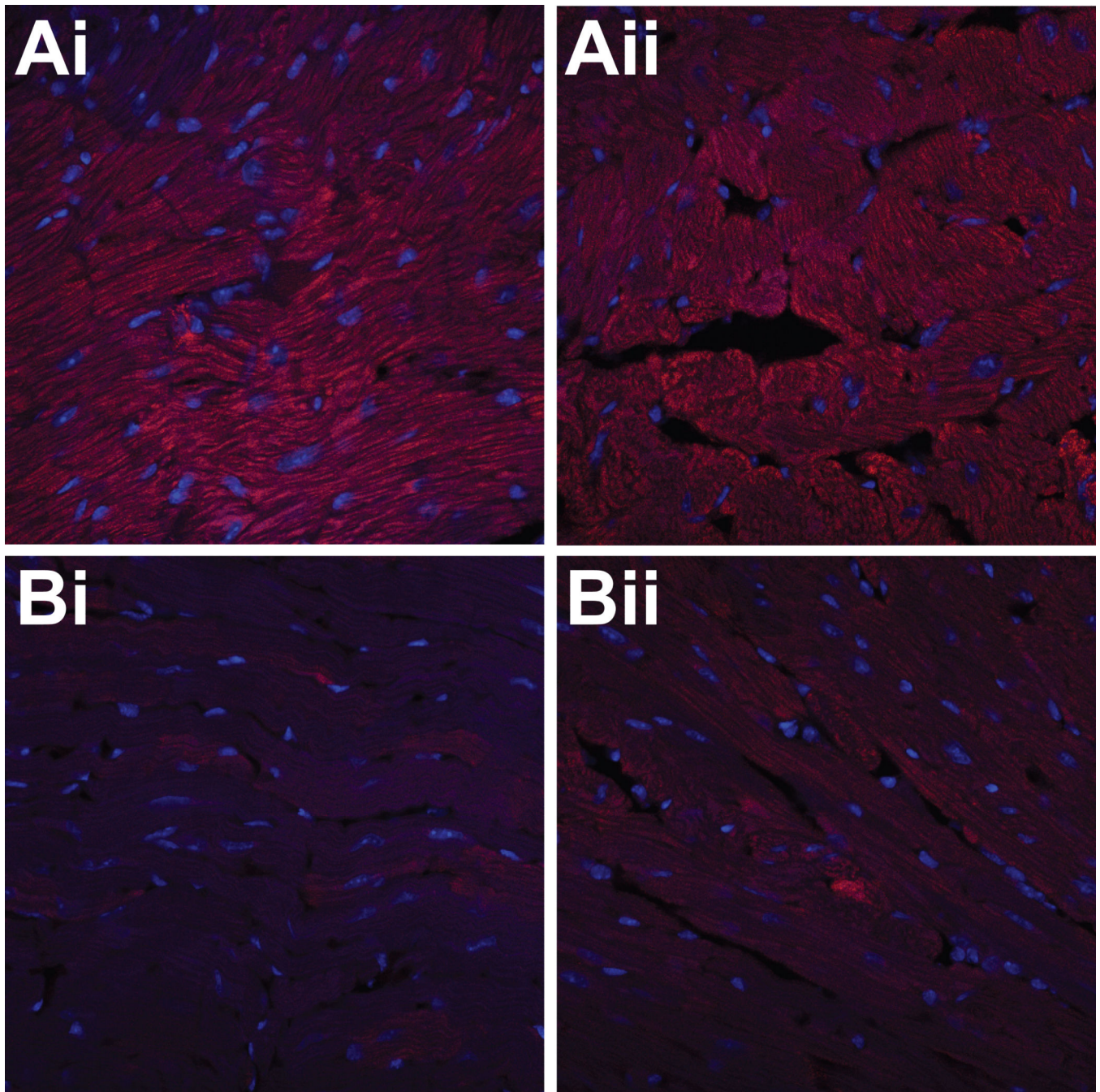


Figure 5.
Ex vivo detection of the anti-DMPO probe in hearts of diabetic mice. Fluorescence images of streptavidin-Cy3 (red) which binds to biotin moiety of anti-DMPO probe in STZ diabetic mouse cardiac muscle (A) and muscle tissue from non-diabetic mice (B).

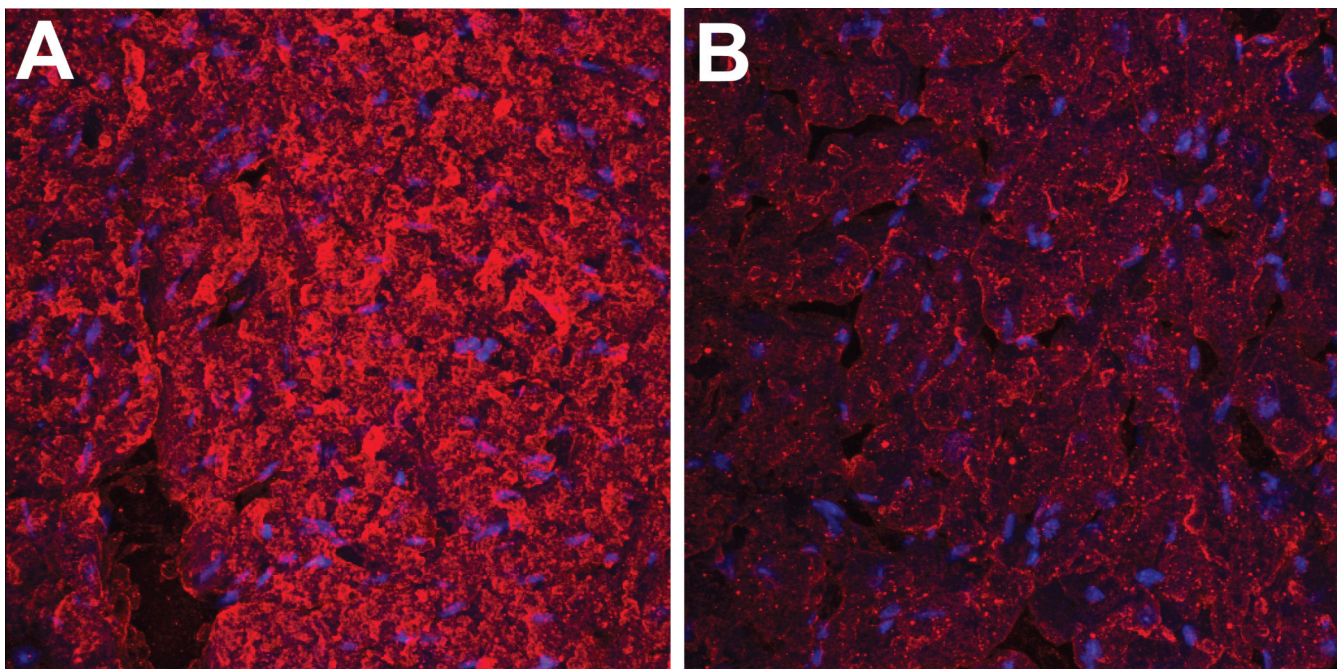


Figure 6.
Ex vivo detection of trapped DMPO-nitron radical adducts in hearts of diabetic mice. Fluorescence images of fluorescent (red)-labeled anti-DMPO antibodies in STZ diabetic mouse cardiac muscle (A) and muscle tissue from non-diabetic mice (B).

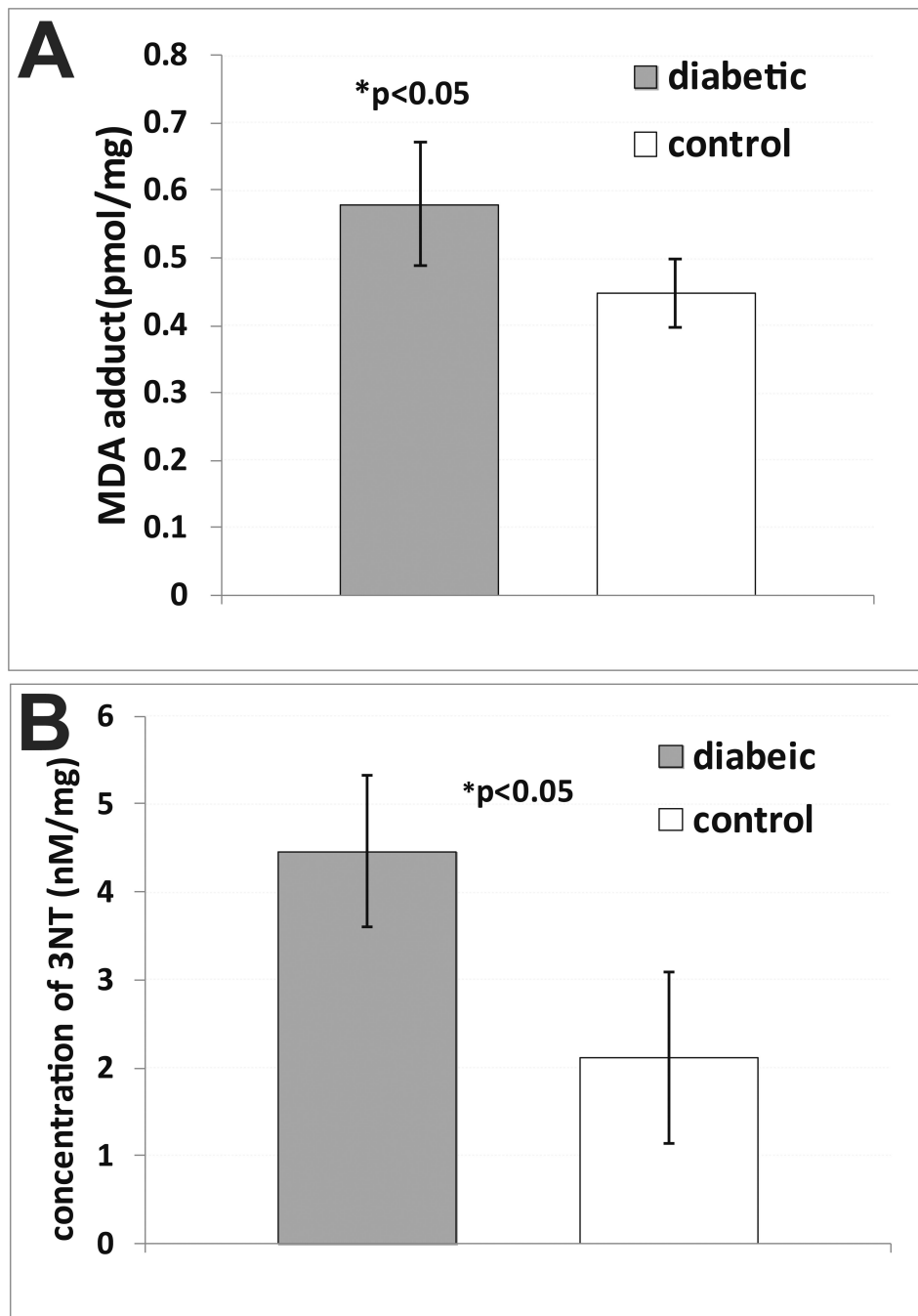


Figure 7. *Ex vivo* detection of oxidative stress in hearts of diabetic mice. (A) Quantitative measure of malondialdehyde (MDA)-protein adduct concentration (pmol/mg protein) in tissues homogenates from diabetic and non-diabetic mouse cardiac muscle (n=5 for each). There was a significant increase in MDA-adducts in diabetic mice ($p < 0.05$) compared to non-diabetic mice. (B) Quantitative measure of 3-nitrotyrosine (3-NT) concentration (nM/mg protein) in tissues homogenates from diabetic and non-diabetic mouse cardiac muscle (n=5

for each). There was a significant increase in 3-NT in diabetic mice ($p < 0.05$) compared to non-diabetic mice.

Author Manuscript

Author Manuscript

Author Manuscript

Author Manuscript